NAVAL POSTGRADUATE SCHOOL

MONTEREY, CALIFORNIA

THESIS

INTEGRATION OF AN ACOUSTIC MODEM ONTO A WAVE GLIDER UNMANNED SURFACE VEHICLE

by

Joseph N. Beach

June 2012

Thesis Advisor: Joseph A. Rice

Approved for public release; distribution is unlimited

THIS PAGE INTENTIONALLY LEFT BLANK

REPORT DOCUMENTATION PAGE			*Form Approved OMB No. 0704–0188*
Public reporting burden for this collection of information is estimated to average 1 hour per response, including the time for reviewing instruction, searching existing data sources, gathering and maintaining the data needed, and completing and reviewing the collection of information. Send comments regarding this burden estimate or any other aspect of this collection of information, including suggestions for reducing this burden, to Washington headquarters Services, Directorate for Information Operations and Reports, 1215 Jefferson Davis Highway, Suite 1204, Arlington, VA 22202–4302, and to the Office of Management and Budget, Paperwork Reduction Project (0704–0188) Washington DC 20503.			
1. AGENCY USE ONLY ***(Leave blank)***	**2. REPORT DATE** June 2012	**3. REPORT TYPE AND DATES COVERED** Master's Thesis	
4. TITLE AND SUBTITLE Integration of an Acoustic Modem onto a Wave Glider Unmanned Surface Vehicle			**5. FUNDING NUMBERS**
6. AUTHOR(S) Joseph N. Beach			
7. PERFORMING ORGANIZATION NAME(S) AND ADDRESS(ES) Naval Postgraduate School Monterey, CA 93943–5000			**8. PERFORMING ORGANIZATION REPORT NUMBER**
9. SPONSORING /MONITORING AGENCY NAME(S) AND ADDRESS(ES) N/A			**10. SPONSORING/MONITORING AGENCY REPORT NUMBER**
11. SUPPLEMENTARY NOTES The views expressed in this thesis are those of the author and do not reflect the official policy or position of the Department of Defense or the U.S. Government. IRB Protocol number ______N/A______.			
12a. DISTRIBUTION / AVAILABILITY STATEMENT Approved for public release; distribution is unlimited			**12b. DISTRIBUTION CODE** A

13. ABSTRACT (maximum 200 words)

This thesis examines the possibility of integrating an acoustic modem onto a Wave Glider with the goal of providing a bidirectional communications gateway for submerged sensors, platforms, and networks. The Wave Glider unmanned surface vehicle continuously harvests energy from the environment and is able to hold station without needing to refuel. A unique two-body architecture and wing system directly converts wave motion into thrust, and solar panels provide electricity for sensor payloads. Data messages are transmitted to shore via satellite, and the continuous surface presence means that data can be delivered in real time as it is collected. The objective of this thesis is to identify the best location for an acoustic modem on the Wave Glider, considering the factors of hydrodynamic drag on the vehicle and acoustic performance of the modem.

14. SUBJECT TERMS Acoustics, sound, ocean, acoustic communications, underwater network, Seaweb, drag, hydrodynamic propulsion, noise, Wave Glider, USV, acoustic modem			**15. NUMBER OF PAGES** 61
			16. PRICE CODE
17. SECURITY CLASSIFICATION OF REPORT Unclassified	**18. SECURITY CLASSIFICATION OF THIS PAGE** Unclassified	**19. SECURITY CLASSIFICATION OF ABSTRACT** Unclassified	**20. LIMITATION OF ABSTRACT** UU

NSN 7540–01–280–5500

Standard Form 298 (Rev. 2–89)
Prescribed by ANSI Std. 239–18

THIS PAGE INTENTIONALLY LEFT BLANK

Approved for public release; distribution is unlimited

INTEGRATION OF AN ACOUSTIC MODEM ONTO A WAVE GLIDER UNMANNED SURFACE VEHICLE

Joseph N. Beach
Ensign, United States Navy
B.S., United States Naval Academy, 2011

Submitted in partial fulfillment of the
requirements for the degree of

MASTER OF SCIENCE IN APPLIED PHYSICS

from the

NAVAL POSTGRADUATE SCHOOL
June 2012

Author: Joseph N. Beach

Approved by: Joseph A. Rice
Thesis Advisor

Andres Larraza
Chair, Department of Physics

THIS PAGE INTENTIONALLY LEFT BLANK

ABSTRACT

This thesis examines the possibility of integrating an acoustic modem onto a Wave Glider with the goal of providing a bidirectional communications gateway for submerged sensors, platforms, and networks. The Wave Glider unmanned surface vehicle continuously harvests energy from the environment and is able to hold station without needing to refuel. A unique two-body architecture and wing system directly converts wave motion into thrust, and solar panels provide electricity for sensor payloads. Data messages are transmitted to shore via satellite, and the continuous surface presence means that data can be delivered in real time as it is collected. The objective of this thesis is to identify the best location for an acoustic modem on the Wave Glider, considering the factors of hydrodynamic drag on the vehicle and acoustic performance of the modem.

THIS PAGE INTENTIONALLY LEFT BLANK

TABLE OF CONTENTS

LIST OF FIGURES

THIS PAGE INTENTIONALLY LEFT BLANK

LIST OF TABLES

THIS PAGE INTENTIONALLY LEFT BLANK

ACKNOWLEDGMENTS

I would like to thank the following people for their encouragement, support, and assistance in completing this thesis:

Firstly, I would like to thank my parents and family for their continued support and encouragement during my time here. They always kept reminding me that I could do anything I put my mind to.

To Joseph Rice, for constantly providing me helpful feedback and suggestions for the entire research and writing process. This project would not have been remotely possible without his assistance.

To my fiancée, Calline Beard, for constantly pushing me to complete the project even when I got stuck. Her constant words of encouragement gave me a level of drive to write this paper that I otherwise would not have.

To Mike Moberg and Rebecca King for helping me transport the Wave Glider for demonstrations and also providing constant support throughout my time at NPS.

To Liquid Robotics and their employees, for providing me technical information about the Wave Glider and allowing me the opportunity to learn about their vehicle.

To Teledyne Benthos and their employees, for providing their views on best possible integration schemes for the modem.

To David Jackson at ONI, for donating a Wave Glider to NPS for research.

To Timothy Rochholz and Pascal Gagnon, for also helping me transport the Wave Glider for demonstrations and giving me advice for my project.

Finally, I would like to thank all of the faculty and staff at NPS for providing me with a very fruitful experience during my time here in Monterey.

THIS PAGE INTENTIONALLY LEFT BLANK

I. INTRODUCTION

A. PROBLEM STATEMENT

Emerging underwater surveillance sensors and sensor networks will facilitate the detection and deterrence of potential threats to homeland security. The NPS Seaweb project currently uses a system of acoustic modems capable of underwater networked communication. A critical node in the Seaweb network is the gateway node located on the ocean surface that connects the underwater nodes to command centers. Gateway nodes usually take the form of a gateway buoy. However, moored gateway buoys can be expensive to maintain and are vulnerable to natural and human threats. This thesis examines an alternate gateway node concept, the incorporation of a networked acoustic modem onto a versatile autonomous marine craft, the Liquid Robotics Wave Glider.

B. OBJECTIVE

The objective of this thesis is to optimize the integration of the acoustic modem onto the Wave Glider. An analysis is presented of the possible drawbacks or positive qualities associated with candidate locations for the modem. Considerations made in this analysis include drag and hydrodynamic performance, effectiveness of acoustic communication, noise limitations, shadowing/interference of the vessel, and availability of power.

THIS PAGE LEFT INTENTIONALLY BLANK

II. BACKGROUND

A. SEAWEB UNDERWATER ACOUSTIC NETWORK

Seaweb is a system of acoustic modems capable of underwater networked communications. The network consists of distributed fixed and mobile nodes as illustrated in Figure 1. The area coverage is scaleable according to the environmental acoustic conditions and the number of available nodes. Typically, the network nodes are expendable, battery-limited, and placed relatively close to the sea floor. This is effective in areas where cabled or buoyed sensor arrays could be subject to dangers such as trawling, tampering, and collisions with ship traffic. Although, the concept of Seaweb has been proven to work, there remain aspects of the capability that are undergoing further improvement. These include situation-adaptive, self-configuring, and self-healing mechanisms to increase the longevity of Seaweb components in situations where autonomy is demanded. The aim of this thesis is to improve the reliability and independence of gateway nodes at the sea surface [1].

Information is transmitted between nodes acoustically underwater until it reaches a gateway node. The gateway node is equipped with a modem that converts the acoustic information into a signal that is transmitted to an Iridium satellite and then redirected to command centers monitoring the observed area. Currently, gateway nodes are buoys that maintain station by using an anchor and swivel system that is moored to the ocean floor. These gateway nodes are the critical interface between the underwater network domain and the above-water satellite and terrestrial domains. Ideally, they are located within the Seaweb network so as to maximize the number of underwater nodes that they can communicate with while also avoiding shore hazards and shipping lanes [1].

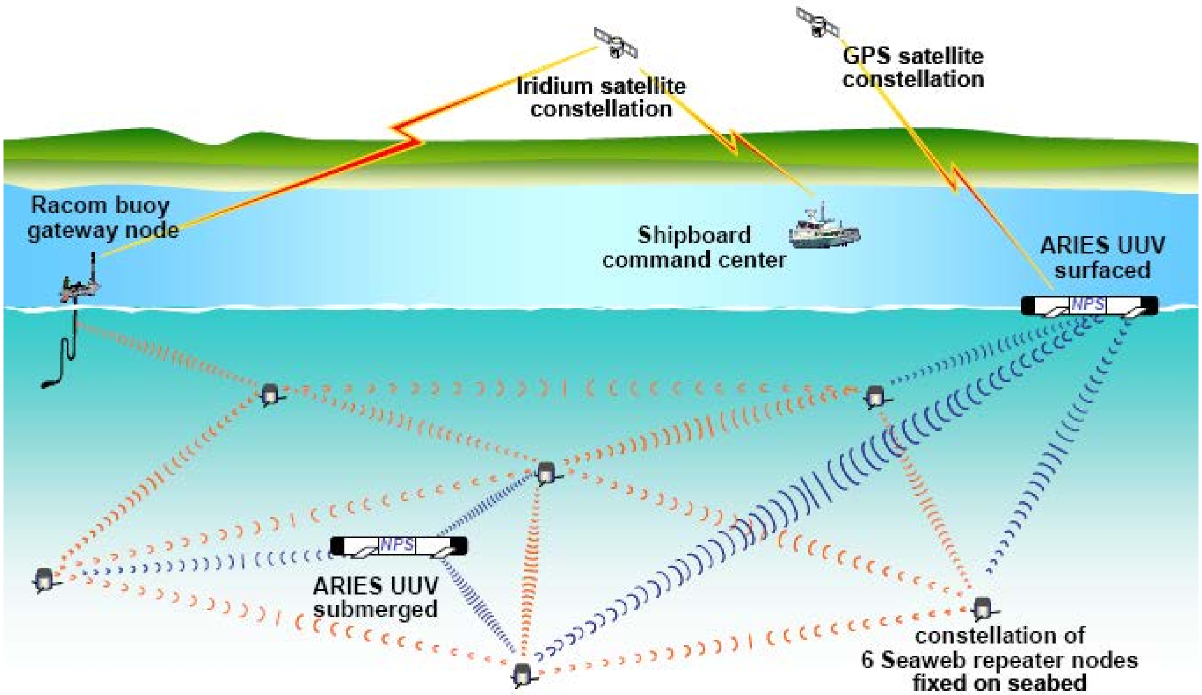

Figure 1. The described Seaweb architecture. Information is collected by fixed and mobile nodes, sent to a gateway node, and then transmitted to a command center via the Iridium satellite constellation.

Currently, these buoys are statically moored and require maintenance. However, what if the modems were attached to an unmanned surface vehicle (USV) that could harness power from the ocean itself to maximize station time and reduce network maintenance? Seaweb engineers have been seeking an appropriate USV for this purpose since 2005 [2]. Incorporating an acoustic modem onto a suitable USV would greatly extend the capabilities of an information gathering underwater network such as Seaweb both in terms of reliability and minimization of maintenance.

B. WAVE GLIDER UNMANNED SURFACE VEHICLE

Liquid Robotics' Wave Glider is a wave-powered USV. By using the vertical motion of the ocean surface, it converts potential energy into forward propulsion in order to make way or maintain station. This is achieved by using a two-body system [3]. The lower body of the vehicle stays completely submerged and consists of six swiveling fins that generate horizontal forward thrust when the vehicle is moved vertically up and down.

The upper body of the Wave Glider uses buoyancy to remain on the ocean surface and pull the lower portion up along with it upon encountering a wave. Using this method of propulsion, the vehicle can achieve up to 2 knots through the water. Clear advantages of this energy-harvesting system include lack of any fuel consumption, long endurance, and relatively little noise to interfere with acoustic communications. There is also an increased stealth capability since the main source of propulsion is 7 meters below the surface of the water. The height of the vehicle above the water is no more than 5 to 10 centimeters [4]. The manufacturer of the Wave Glider refers to the upper body as the "float" and the lower body as the "glider." These terms will now be used in reference to the two different bodies.

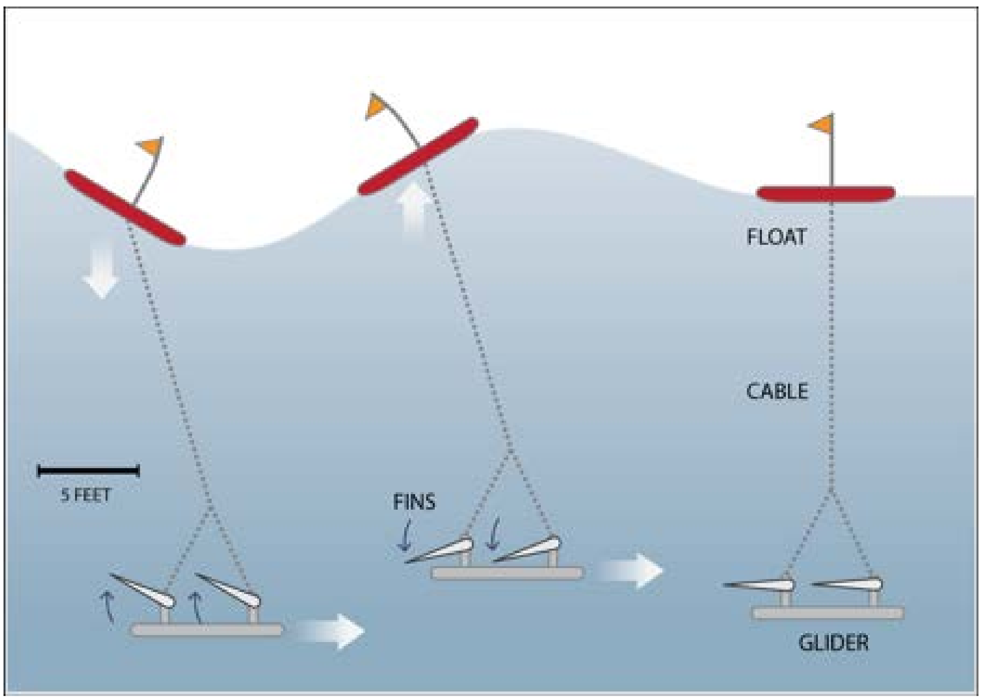

Figure 2. Potential energy from changes in elevation of the Wave Glider is converted into thrust at the glider portion of the vehicle.

The vehicle is equipped with solar panels on the float that can provide up to 80W of hotel power to onboard electronics or other instruments requiring power. Excess solar energy is stored in a battery, as a reserve for night operations and occurrences of high demand. The solar energy system has ample capacity to power an acoustic modem [4].

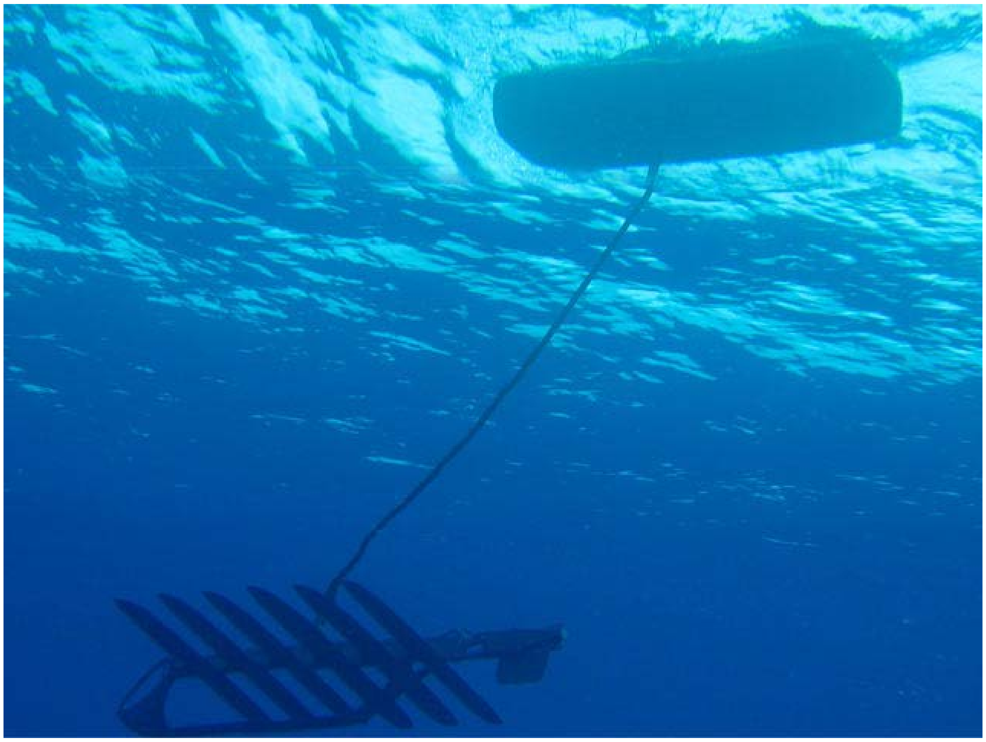

Figure 3. A Wave Glider in operation. The float is attached to the glider via a 7-meter tether.

In terms of survivability in harsh weather conditions, the Wave Glider also excels. The vehicle was tested in Hurricane Flossie in 2007 and was able to survive 10-foot seas and 40-knot winds. While there is a limit to making way in increasingly rough sea states because of strong currents and multidirectional waves, fairly high sea states will actually help in terms of maintaining station, since vertical motion is the vehicle's main source of propulsion [4].

Integrating an acoustic modem onto the Wave Glider presents several challenges. These include minimization of noise, reduction of drag, and identifying a preferable location for acoustic communications performance. The acoustic modem could be placed underneath the upper body of the Wave Glider, on the lower body of the Wave Glider, or it could be placed in a separate tow body, which would be attached by a tow to the glider. Each of these possibilities has advantages and disadvantages in the considerations for placement mentioned earlier, and the goal was to identify which location was the most advantageous.

III. INTEGRATION OF THE ACOUSTIC MODEM

A. PLACEMENT OPTIONS

1. Mounted underneath the Float

The float portion of the vehicle is made of fiberglass and is easily modified. For mounting an instrument on the underside of the float, a hole could be cut into the body, and the equipment could be fitted inside. This has an advantage of minimizing the cross-sectional area of the sensor or instrument that would be exposed to drag forces. However, if the sensor is acoustical in nature, as is our modem, it has the disadvantage of being close to the surface. This makes it more susceptible to noise. Another advantage is the direct access to power and to the onboard electronics in the payload bays within the float.

Some instruments have previously been integrated into the Wave Glider float. In one experiment, Teledyne Benthos and Liquid Robotics were interested in integrating an Acoustic Doppler Current Profiler (ADCP) with the vehicle in order to collect current measurements near the surface of the water. A hole was cut in the hull of the float and the ADCP was mounted in it. A fairing was also constructed around the ADCP in order to reduce the drag associated with it. This integration can be seen in Figure 4 [5].

Figure 4. An Acoustic Doppler Current Profiler mounted to the float. The streamlined shape was used to reduce drag.

2. Mounted on the Glider

Mounting the modem on the glider has the advantage of being away from ocean turbulence, bubbles, and noise. However, unlike the float, there is no existing volume for encapsulating the modem and hence reducing the cross-sectional area that would be presented to the flow field. Thus, the amount of drag created due to the modem would increase in this scheme. Also, all of the vehicle's propulsion is generated from the glider portion of the vehicle. Attaching more mass onto the glider without accounting for the shift in the center of gravity and other hydrodynamic properties of the vehicle might severely impact the efficiency of the propulsion system. Lastly, wiring would have to be implemented in order to connect the modem to the instrumentation and power source located on the float.

Integration schemes where instrumentation is attached to the glider section have already been used in multiple experiments. While thus far the integration has been crude with respect to minimization of drag, usually it meets the needs for the experiment being carried out at the time. One such integration is shown in Figure 5. In this experiment, an active transducer and a passive hydrophone were placed on the tail end of the glider body. No effort was made to streamline the transducer or integrate it into the structure of the glider [6].

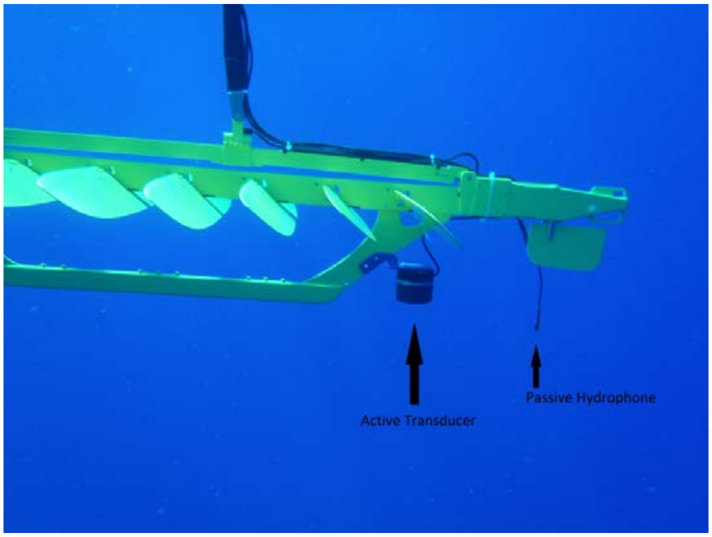

Figure 5. An experiment in which an active transducer and a passive hydrophone were mounted onto the glider.

3. Pulled in a Tow Body

The tow-body configuration has many appealing characteristics about it compared with the latter two configurations. It has both the advantages of being away from the surface of the water, and being completely customizable in terms of shape in order to minimize drag. One would think that the extra cable connecting the tow body to the glider would produce a significant drag on its own. However, a mechanically compliant, low-drag cable has been developed to mitigate this issue. The biggest disadvantage with a tow body is the increased handling complexity. Deployment and recovery operations at sea will be more difficult and more risky with a three-body configuration.

In March 2012, Cornell, BioSonics, and Liquid Robotics worked together to perform some tests on a BioSonics dual-frequency echosounder. In this experiment, a Wave Glider pulled a tow body housing a 70 kHz and 200 kHz transducer. In Figure 6, we can see the tow body [7].

Figure 6. The Wave Glider and the tow body used in the dual-frequency echosounder experiment off the coast of Hawaii.

4. Separation of Receiver and Transmitter

Another possibility that was considered but not analyzed in this thesis is that of separating the transmitter and receiver portions of the modem. The larger transmitter could be placed underneath the float and gain the benefit of minimized cross-sectional area. The receiver would be placed on the glider or in a towed hydrophone array to avoid surface noise. This complicates the integration because of the separation of modem parts, additional wiring required, and delivery of power. However, it should still be examined in future research.

B. INTEGRATION CONSIDERATIONS

1. Drag

The complete configurability of the tow body means that we could optimize the shape to reduce its associated drag. It will be informative to estimate how much drag would be produced from placing the transducer on either the glider body or the float in order to quantify the advantage of placing the modem in the tow body. In Chapter IV, a description is given of the approximations and theory used to provide an estimate of this advantage.

2. Acoustic Communications

It would also be helpful to identify what impact the depth of the sensor would have on the acoustic propagation path to a node below it. Also of interest is whether or not a modem mounted on the float would encounter problems due to the glider being beneath the sensor at some angle. In Chapter V, an analysis of ray theory is given along with some propagation modeling using Bellhop and Matlab.

3. Noise

Lastly, we wish to estimate how much noise is associated with each modem location at the frequencies of interest. As mentioned previously, the float configuration would be subject to surface noise that would be lessened by placing the modem deeper in the water. An analysis of different sources of noise and their impact on the system is provided in Chapter VI.

IV. DRAG CONSIDERATIONS

A. BACKGROUND

1. Drag Coefficient

An object moving through a fluid at any velocity experiences a resistive force known as drag. Drag is caused by the pressure and shear stress distributions on an object due to a particular fluid's viscosity and flow characteristics. If the pressure and shear stress distributions over the object are known, one would simply integrate the pressure and shear stress distributions over the surface area of the object in order to obtain the net force acting in the opposite direction of the velocity. However, most of the time, these distributions are not known, and empirical data must be used in order to solve for the drag forces on the object. Typically, this is done by using a dimensionless quantity known as the drag coefficient. The drag coefficient is defined by

(4.1)
$$c_D = \frac{F_D}{\frac{1}{2}\rho A V^2}$$

Here F_D is equal to the drag force, ρ is the density of the fluid, V is the velocity of the object relative to the fluid, and A is the characteristic area of the object (usually the frontal area or the surface normal to the direction of flow) [8].

Sometimes the drag coefficient is separated into two component coefficients.

(4.2)
$$c_D = c_{Df} + c_{Dp}$$

The first component is the coefficient of drag due to friction and the second is the coefficient of drag due to pressure. Friction effects are more noticeable when the viscosity of the fluid is high and there is a lot of shear stress acting on the object while the pressure drag is more strongly dependent on the shape or form of the object. Depending on the fluid that an object is in, the drag coefficient can have very different values [9].

To assess the increased drag caused by adding an acoustic modem onto the Wave Glider, we approximate the acoustic modem as a cylinder in incompressible fluid flow. It should be noted that this analysis applies to the case where the modem is mounted without any fairing.

2. Drag Coefficient of a Cylinder in Viscous Incompressible Flow

Most information relating to drag has been attained by conducting numerous flow experiments on the object of interest. The exact size and shape of the modem we plan to use are not available. However, we can approximate its dimensions and draw some conclusions as to its drag characteristics.

We approximate the acoustic modem as a cylinder. The drag coefficient for a cylinder in incompressible flow normal to the axis can be found in a table or book. The drag coefficient for a cylinder in incompressible flow is

$$c_D = c_{Df} + c_{Dp} = \frac{5.93}{\sqrt{\mathrm{Re}}} + 1.17 \tag{4.3}$$

Here, the drag coefficient is expressed as a function of the Reynolds number. The Reynolds number is a dimensionless quantity that describes the ratio of inertial effects to viscous effects [9].

$$\mathrm{Re} = \frac{\rho V L}{\mu} \tag{4.4}$$

Here, ρ is the density of the fluid, V is the velocity of the object relative to the fluid, L is the traveled length of the fluid, and μ is the dynamic viscosity of the fluid. So in order to figure out the coefficient of drag, we must first calculate the Reynolds number of seawater. Plugging in all of the values for seawater, assuming that the traveled length of the fluid is half the circumference of our cylinder, and assuming a velocity of 1 knot we get a Reynolds number of 77000 (a large Reynolds number). This is to be expected, because seawater is not very viscous. Therefore, there is negligible friction drag in our analysis. Pressure drag dominates, and we are able to make assumptions based on very high Reynolds number flows. If we look at our coefficient of drag now, the friction component is negligible, because the Reynolds number is so large.

(4.5) $$c_D = 1.17$$

This also assumes though that the cylinder is infinitely long in a 2 dimensional fluid flow. In Figure 7, we can see that the coefficient of drag of a cylinder depends on the aspect ratio of the cylinder [10]. For our modem, let us assume that the length of the cylinder is approximately 1.5 times that of the diameter.

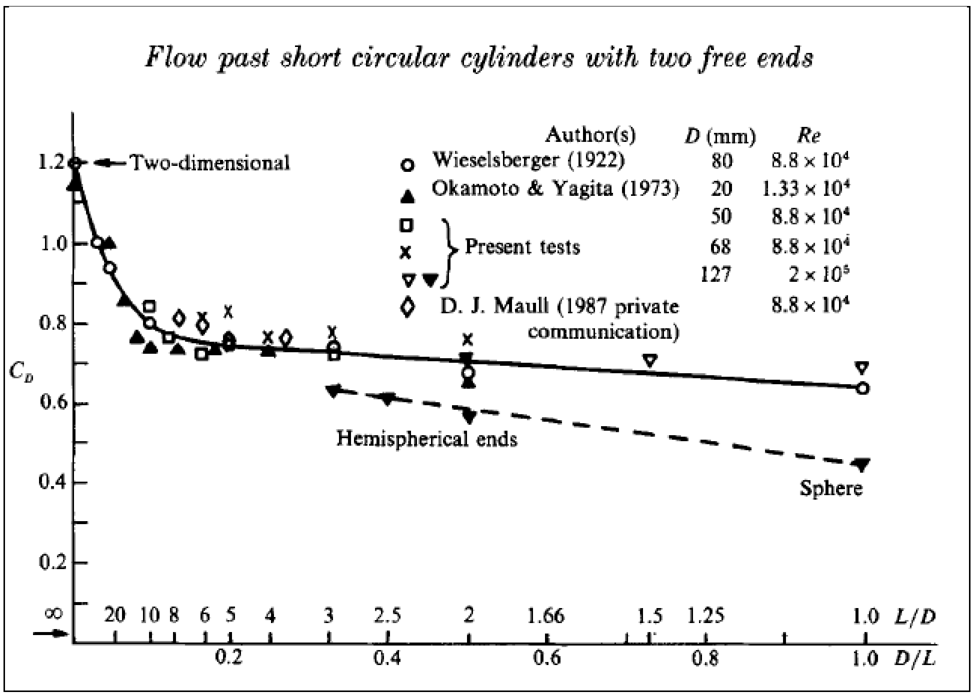

Figure 7. A graph relating the aspect ratio of a cylinder with two free ends to its drag coefficient. We can see that as the length of the cylinder becomes greater than its diameter, the drag coefficient approaches the value 1.17.

Thus our new coefficient of drag becomes smaller.

(4.6) $$c_D \cong 0.7$$

3. Drag Force of Acoustic Modem in Seawater

Now that we have an approximate coefficient of drag for the modem we can get an approximation for the drag force exerted on it while it moves through the water. The previously mentioned equation of drag can be rearranged to solve for the force.

$$F_D = \frac{1}{2}\rho c_D A V^2 \tag{4.7}$$

If we plug in values on the right side of the equation, we obtain the drag force associated with adding a modem to the vehicle, depending on the amount of exposed area and the speed at which the vehicle is traveling. However, this does not help us calculate the reduction in speed experienced by the vehicle until we know the amount of thrust generated by the propulsive system of the Wave Glider.

B. ANALYSIS OF WAVE GLIDER PROPULSION SYSTEM

1. Previous Work

Work has been done previously quantifying the force of thrust of a wave propelled vehicle as a function of wave height and period [11]. Using a wave tank and a cable attached to a force meter, one can measure the tension in the cable and obtain values for the thrust of the vehicle as the wave height and period in the tank is adjusted. This approach was considered in this analysis as viable method of determining a reduction in speed of the Wave Glider. However, here we limit ourselves to a theoretical estimate based on the power of ocean waves and power/thrust relations.

2. Power Generated by Ocean Waves

The amount of thrust generated by the Wave Glider is dependent on the changes in potential energy associated with the vertical displacement of the float. This is converted into forward thrust by the flapping motion of the fins on the glider body. The theoretical amount of power in a monochromatic deep ocean wave is a function of the wave height *H*, and the wave period *T*.

$$P_{wave} = \frac{\rho g^2 H^2 T}{32\pi} \text{ [W/m]} \tag{4.8}$$

Here ρ is the density of seawater, and g is the acceleration due to gravity. This is actually the power of the wave per meter of crest length [12]. Crest length is a measurable parameter related to the spectral density of the ocean waves [13]. Many studies have gone into producing distributions of wave crest length in the ocean under different weather and sea conditions. For the purposes of this study, I will approximate the length of the wave crest as the speed at which the Wave Glider is traveling multiplied by the wave period, since the order of wave crests length is comparable to that of the wave length [14]. We now have a new equation for the power of each wave.

$$\Pi_{wave} = \frac{\rho g^2 H^2 T^2 V}{32\pi} \text{ [W]} \tag{4.9}$$

The vehicle is of course not able to use all of this power for thrust as nothing is 100% efficient. The next step in finding the thrust generated is to estimate the efficiency of the vehicle.

3. Wave Glider Propulsion Efficiency

Flapping foil motion used for propulsion is actually very efficient when compared to other methods of propulsion. Much research is still being conducted on how certain birds, fish, and insects are able to swim/fly so much more efficiently than some of the propellers in use today. The reason it is not used for everything is because it is somewhat limited in the amount of thrust that it can produce. Higher levels of thrust can be generated; however, much of the efficiency is sacrificed. The efficiency of the flapping foil can be characterized as a function of the Strouhal number, the heave amplitude, the angle of attack of the foil, and the phase angle between the pitch and the heave. In Figure 8, a graph shows the different contours of the efficiency of a flapping foil as a function of the angle of attack and the Strouhal number [15].

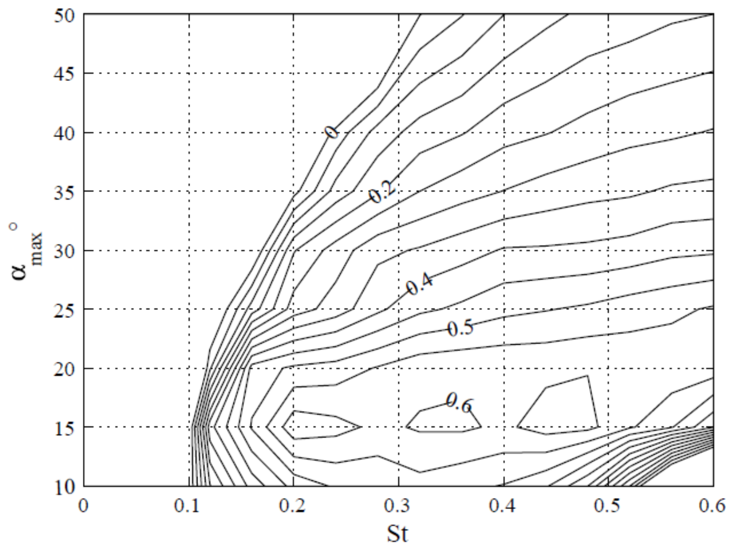

Figure 8. A contour plot of the efficiency of an airfoil with a given ratio between the heave amplitude h_o and the chord length c

Using some of the empirical data from this particular study, we can find an approximation to the propulsive efficiency of the Wave Glider once we know values for a couple of the parameters. The first one we can find is the Strouhal number. The Strouhal number is a function of the heave amplitude h_o, the angular frequency of the flapping foil ω, and the velocity of the foil V (or in this case the speed of the Wave Glider) [14].

$$\mathrm{St} = \frac{4\pi h_o \omega}{V} \tag{4.10}$$

We can calculate the Strouhal numbers for our vehicle by using average speeds in various sea states. These sea states also correspond to the wave heights experienced by the vehicle and therefore to the heave amplitude. Lastly, the angular frequency with which the foils oscillate should be related to the period of the waves according to $\omega = 2\pi/T$. Typically, wave periods in the ocean range from 6–20 seconds [12], so let us use a value of T = 6 seconds for the wave period and thus the angular frequency of the oscillating foils is $\pi/3$ [rad/s]. Table 1 shows the average speed of the wave glider in varying sea states [4]. I have adjusted the table so that it also shows the wave heights corresponding to those sea states (using the Douglas Sea Scale) and the average speed in meters per second.

Sea State	Wave Height (m)	Wave Glider Speed (knots)	Wave Glider Speed (m/s)	Oscillating Frequency (rad/s)	Strouhal Number
Flat Calm	0.00	0.00	0.00	1.05	0.00
Sea State 0	0.01	0.38	0.19	1.05	0.68
Sea State 1	0.05	1.00	0.51	1.05	1.28
Sea State 2	0.30	1.63	0.84	1.05	4.72
Sea State 3	0.88	1.88	0.96	1.05	11.94

Table 1. Data relating the speed of the Wave Glider to the sea state. A wave period of 6s is assumed thus producing an oscillating frequency of $\omega = 1.05$ rad/s Strouhal numbers were calculated from each corresponding heave amplitude (wave height), speed of the wave glider, and oscillating frequency.

Unfortunately, the study of efficiency of flapping foils did not go to higher Strouhal numbers [15], and the ratio between the heave amplitude and the chord length was kept to 1. Although our heave amplitudes are much greater than the chord length of our foils, I decided to extrapolate from their data to estimate the efficiency of the vehicle. The Strouhal number derived from the sea state 0 value in Table 1 is 0.68 and the angle of attack of the foils of the wave glider is around 40°. Using these values and the contour plot in Figure 8, I approximated the net efficiency of the wave glider to be around $\eta = 0.45$.

4. Wave Power Utilized by the Wave Glider

Now that we have a rough estimate of the efficiency of the Wave Glider and the power contained within an ocean wave of a given height, we can approximate the power available for forward thrust. We simply multiply the efficiency of the system by the power of the wave to get the motive power of the Wave Glider. Table 2 takes the values for wave height from Table 1 and lists the power associated with these wave heights by using Equation (4.8) (once again assuming a wave period of 6 seconds). These values are then multiplied by the efficiency of the Wave Glider to get the power available for thrust.

Sea State	Wave Height (m)	Wave Glider Speed (m/s)	Power of Ocean Waves (W)	Efficiency of Wave Glider η	Power Available for Thrust (W)
Flat Calm	0.00	0.00	0.00	0.45	0.00
Sea State 0	0.01	0.19	0.680	0.45	0.306
Sea State 1	0.05	0.51	45.3	0.45	20.4
Sea State 2	0.30	0.84	2650	0.45	1190
Sea State 3	0.88	0.96	26000	0.45	11700

Table 2. Values for the Wave Glider's available thrust are calculated using the power available in an ocean wave of the indicated height and the approximate efficiency of the Wave Glider.

5. Drag and Thrust Forces of the Wave Glider

Using some basic mechanics, we can now calculate the drag and thrust force of the Wave Glider by using the power values that we just calculated. For propulsion there is a relation between the thrust force, velocity of the vehicle, and the power of the propulsion [16].

$$\Pi_{WG} = F_{Thrust} V \tag{4.11}$$

Assuming that the velocity of the Wave Glider is approximately constant in these sea state conditions, we divide the power by the speed of the Wave Glider to find the thrust force. We should also note though that since the vehicle is going at a constant speed and not accelerating, there can be no net forces acting on the vehicle. Figure 9 shows a free-body diagram of the Wave Glider [6].

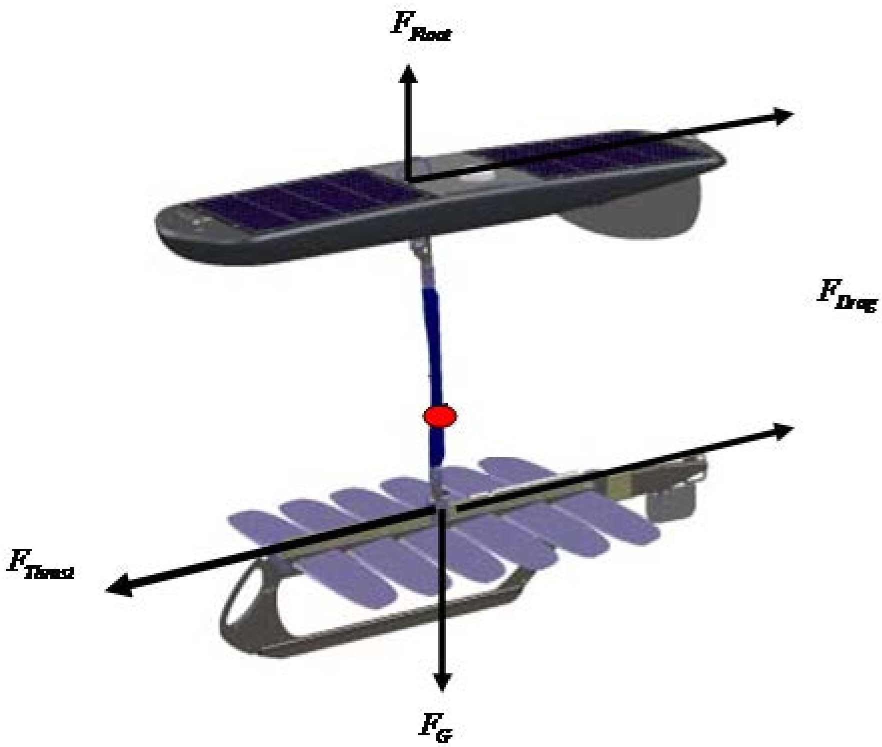

Figure 9. A free-body diagram with the forces acting on the Wave Glider

This means that the magnitude of the force of drag must be equal to the thrust force. This is important, because based on the speed it is going we can use Equation (4.7) to calculate the coefficient of drag.

(4.12) $$0 = F_{net} = F_{Thrust} + F_{Drag}$$

(4.13) $$\left|F_{Thrust}\right| = \left|F_{Drag}\right|$$

6. Coefficient of Drag of the Wave Glider

Since we know the thrust force, we can set it equal to the drag force. We then use Equation (4.1) to solve for the drag coefficient. Table 3 shows the values for the thrust and drag forces and the coefficient of drag. The frontal area of the vehicle was approximated at 0.060 m^2 by using dimensions provided by a Liquid Robotics specifications sheet and some measurements of my own. These area measurements assumed an ideal case in which the Wave Glider was perfectly level.

Sea State	Power Available for Thrust (W)	Wave Glider Speed (m/s)	Thrust and Drag Force(N)	$\frac{1}{2}\rho AV^2$	Coefficient of Drag of Wave Glider
Flat Calm	0.00	0.00	0.00	0.00	n/a
Sea State 0	0.306	0.19	1.59	1.14	1.39
Sea State 1	20.4	0.51	39.7	8.14	4.87
Sea State 2	1190	0.84	1430	21.5	66.4
Sea State 3	11700	0.96	12100	28.6	425

Table 3. Estimates for the Coefficient of Drag of the Wave Glider

The coefficient of drag should be relatively constant since the only parameters that are changing in our model are the power of the wave and the speed of the wave glider. Unfortunately, as we can see from Table 3, our results are not consistent with this expectation. The disagreement probably results from us using an overly simplistic model for the power of each wave and assuming that the efficiency of the vehicle is constant as the wave height and the speed of the Wave Glider increase. Also, wave heights associated with different sea states can vary quite a bit. Although some of our estimates for the coefficient of drag seem quite far off, our estimates for the coefficient of drag resulting from the data associated with sea state 0 seem to be fairly reasonable. Thus we will use the coefficient of drag value from sea state 0 in all of our future calculations.

(4.14) $$c_D \cong 1.39$$

C. CALCULATING REDUCTION IN WAVE GLIDER SPEED

1. Using Power, Drag, and Thrust Relations to Find Speed Reduction

To find the reduction in speed, we start with Equation (4.11) and realize once again that the thrust force will be equal to the drag force once the Wave Glider reaches a constant speed.

(4.15) $$\Pi_{WG} = F_{Thrust}V = F_{Drag}V$$

This drag force is the sum of drag forces from the modem or the tow body, the drag force from the umbilical cable and the drag forces on the Wave Glider.

(4.16) $$\Pi_{WG} = \left(F_{WG} + F_{Modem} + F_{Cable}\right)V$$

We then also plug Equation (4.7) into Equation (4.16) for each of the drag forces.

(4.17) $$\Pi_{WG} = \left(\frac{1}{2}\rho c_{WG} A_{WG} V^2 + \frac{1}{2}\rho c_{Modem} A_{Modem} V^2 + \frac{1}{2}\rho c_{Cable} A_{Cable} V^2\right)V$$

We can factor out $\frac{1}{2}\rho V^3$.

(4.18) $$\Pi_{WG} = \frac{1}{2}\rho V^3 \left(c_{WG} A_{WG} + c_{Modem} A_{Modem} + c_{Cable} A_{Cable}\right)$$

Now we can solve for the new velocity of the vehicle with the modem added, provided that we also know the coefficients of drag and cross-sectional areas of both the modem and the Wave Glider.

(4.19) $$V = \left[\frac{2\Pi_{WG}}{\rho\left(c_{WG} A_{WG} + c_{Modem} A_{Modem} + c_{Cable} A_{Cable}\right)}\right]^{(1/3)}$$

2. Wave Glider Velocity after Mounting underneath the Float

If the modem is mounted underneath the float without any fairing, most of the cross-sectional area is not exposed to the flow field. Since we assumed earlier that the modem is about 1.5 times as long as its diameter, let us use a length of 15 cm and a diameter of 10 cm to approximate the modem. Since we are analyzing the situation where it is mounted on the float, let us also assume that ¼ of the modem is exposed. This makes the frontal area of the modem equal to a plane of 3.75 cm by 10 cm. Figure 10 shows the geometry.

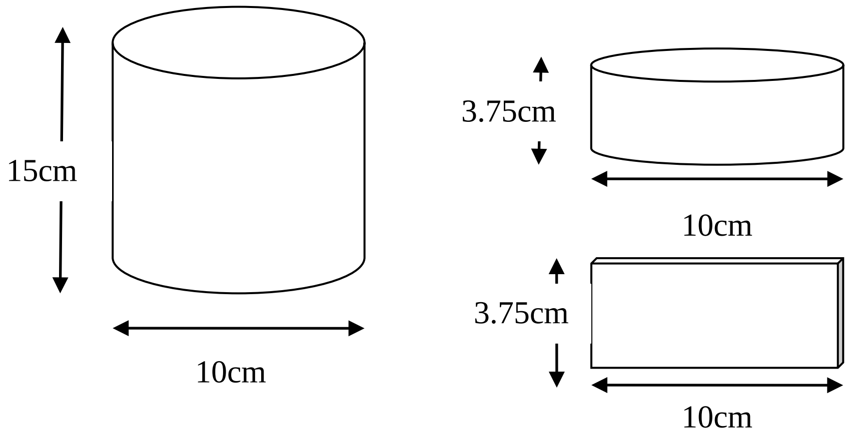

Figure 10. Twenty-five percent of the Cylinder is exposed. Also the frontal area of the cylinder can be considered to be a plane of equal dimensions.

Now we have frontal areas and coefficients of drag for both the wave glider and the partially exposed modem. Also, the drag coefficient of the faired cable is 0.12 [9] and the cross-sectional area is 0.07m^2. Table 4 shows these values and the resulting value of $\left(c_{WG}A_{WG} + c_{Modem}A_{Modem} + c_{Cable}A_{Cable}\right)$.

$\left(c_{WG}A_{WG} + c_{Cable}A_{Cable}\right)$	**Area of Modem (m²)**	c_D **of Modem**	$\left(c_{WG}A_{WG} + c_{Modem}A_{Modem} + c_{Cable}A_{Cable}\right)$
0.0916	**0.00375**	**0.7**	**0.0942**

Table 4. New values for the frontal surface area and drag coefficients are calculated for a float-mounted modem.

To find the reduction in speed, we use Equation (4.19), the values for power available for thrust in Table 3, and the final value for $\left(c_{WG}A_{WG} + c_{Modem}A_{Modem} + c_{Cable}A_{Cable}\right)$ in Table 4. As mentioned previously, since we are using the coefficient of drag value for the Wave Glider corresponding to sea state 0, we should also use the power and initial speed values for sea state 0 as well. The 3rd column of Table 5 is the result of using Equation (4.19) to find the new resultant speed, and the 4th column indicates the percentage reduction of speed.

Power Available for Thrust (W)	Speed Without Modem (m/s)	Calculated Speed With Modem (m/s)	% Reduction in Speed
0.306	**0.193**	**0.185**	**4.11%**

Table 5. The reduction in speed of a float-mounted modem at sea state 0.

A 4.11% reduction in speed is not a tremendous penalty. This could be reduced further if a fairing was constructed around the modem. If our main concern for integration is drag, a float mounted modem is a viable option.

3. Wave Glider Velocity after Mounting on Glider

To calculate the reduction in speed of mounting the modem to the glider, we use the same process illustrated in the last section. The only difference is that now the modem is considered to be fully exposed to the water. The frontal area of the cylinder is now a plane of 15 cm by 10 cm. The geometry is shown by Figure 11.

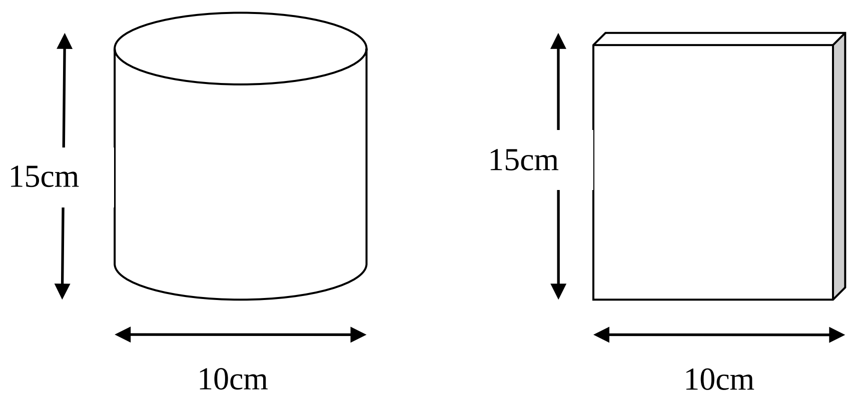

Figure 11. This time, the modem is fully exposed. Once again, the frontal area of the cylinder can be considered to be a plane of equal dimensions.

New values for the area and coefficient of drag are reflected in Table 6.

$\left(c_{WG}A_{WG} + c_{Cable}A_{Cable}\right)$	**Area of Modem (m²)**	c_D **of Modem**	$\left(c_{WG}A_{WG} + c_{Modem}A_{Modem} + c_{Cable}A_{Cable}\right)$
0.0916	**0.015**	**0.7**	**0.102**

Table 6. New areas and coefficients of drag are calculated for the glider-mounted modem.

Finally, the value of $\left(c_{WG}A_{WG} + c_{Modem}A_{Modem} + c_{Cable}A_{Cable}\right)$ is used to calculate the reduction in speed. Once again I used the power values and initial speed values from sea state 0. Table 7 shows the calculated reduction in speed from a glider mounted modem.

Power Available for Thrust (W)	**Speed Without Modem (m/s)**	**Calculated Speed With Modem (m/s)**	**% Reduction in Speed**
0.306	**0.193**	**0.180**	**6.64%**

Table 7. The reduction in speed of a glider-mounted modem at sea state 0.

While still not a tremendous reduction in speed, it is still more than the float mounted case. However, it should be noted that this does not take into account changes in the efficiency of the vehicle due to the modem being mounted on the same portion of the vehicle that provides all of the propulsion. More serious reductions in speed could possibly occur if the modem were not placed near the center of gravity of the vehicle or if it somehow inhibited the Wave Glider's method of harvesting wave energy.

4. Wave Glider Velocity after Adding a Tow Body

Most tow bodies being developed today have a bullet shaped profile in order to minimize drag. Figure 12 shows an approximate shape for a tow body.

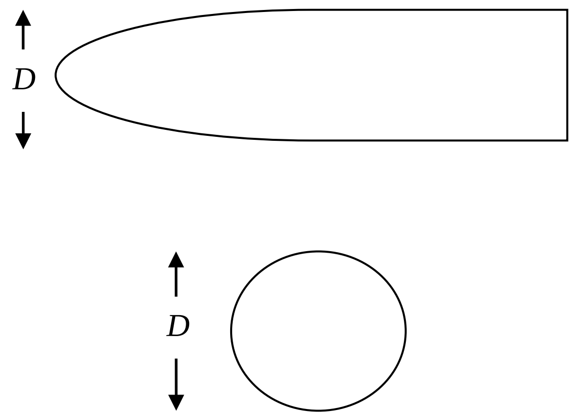

Figure 12. The side and front profiles for an approximate tow body

We will consider a tow body with a diameter that is big enough to house the modem with D =18 cm. The coefficient of drag for such a shape is approximately $c_D = 0.30$ and the frontal area is the area of a circle of diameter D [9]. Using the same process as the previous two sections, we calculate the reduction in speed. Table 8 shows the new total frontal areas and drag coefficients.

$(c_{WG}A_{WG} + c_{Cable}A_{Cable})$	**Area of Tow Body (m²)**	c_D **of Tow Body**	$(c_{WG}A_{WG} + c_{Modem}A_{Modem} + c_{Cable}A_{Cable})$
0.0916	**0.025**	**0.3**	**0.0991**

Table 8. Frontal area and coefficient of drag values after adding a tow body

Again, these values are then used to calculate a reduction in speed. Table 9 shows the results.

Power Available for Thrust (W)	**Speed Without Modem (m/s)**	**Calculated Speed With Modem (m/s)**	**% Reduction in Speed**
0.306	**0.193**	**0.182**	**5.7%**

Table 9. The reduction in speed of a modem mounted inside a tow body.

This configuration lies in between the float-mounted and glider-mounted cases. The tow body may impact the Wave Glider’s propulsive system. In addition, small amounts of drag could be induced by the cable connecting the tow body to the glider, but the hydrodynamics of the tow body can be improved by incorporating compliance and fairing into the tow cable.

D. SUMMARY

From our analysis, the best integration in terms of drag is a modem mounted underneath the float body. The reductions in speed for each case are shown in Table 10.

Integration Scheme	% Reduction in Speed
Float-Mounted	**4.1%**
Glider-Mounted	**6.6%**
Tow-Body Mounted	**5.7%**

Table 10. Comparative reductions in speed for the 3 different integration schemes

As mentioned previously the float mounted reduction in speed could be improved by constructing a fairing around the modem. It would seem that the glider mount is disadvantageous in all respects. Both the float mount and tow-body mount avoid the issue of interfering with the Wave Glider’s propulsion and have favorable values for reduction of speed.

It has been noted that these values seem low compared to test results already carried out. In one particular test in a Liquid Robotics test facility in Kwaihea, Hawaii, the Wave Glider suffered a 20% vehicle-speed reduction compared to an unloaded vehicle [17]. Possible errors in our analysis may arise due to our approximated ocean conditions, namely the wave period and wave crest lengths. Regardless, the hierarchy of the values that we calculated seems reasonable.

V. ACOUSTIC COMMUNICATIONS

A. RAY PROPAGATION THEORY

1. The Wave Equation

Similarly to waves in other media, acoustic waves of small enough amplitude in water obey the linear wave equation. In terms of pressure, *p*, the spatial coordinates *x*, *y*, and *z*, the wave speed *c*, and time *t*, the wave equation can be expressed as

(5.1) $$\frac{\partial^2 p}{\partial t^2} = c^2 \left(\frac{\partial^2 p}{\partial x^2} + \frac{\partial^2 p}{\partial y^2} + \frac{\partial^2 p}{\partial z^2} \right)$$

One way to solve the wave equation is called ray theory. It is useful for understanding an acoustic wave's phase and "position" in terms of space and time. Although waves cannot actually have a position, it is much easier to visualize how a wave propagates in a particular medium by using ray theory [18].

Without going into too much detail, we will briefly describe how one goes from the wave equation to ray theory. First, we use separation of variables to go from the wave equation to the time-independent Helmholtz equation. Note that the spatial derivatives in Equation (5.1) have been condensed into ∇^2 and *x*, *y*, and *z* into *r*.

(5.2) $$\nabla^2 p\left(\vec{r}\right) + k^2\left(\vec{r}\right) p\left(\vec{r}\right) = 0$$

Next, we plug in an ansatz solution to the Helmholtz equation.

(5.3) $$p\left(\vec{r}\right) = A\left(\vec{r}\right) e^{-i\omega\tau\left(\vec{r}\right)}$$

Here $A(r)$ represents the amplitude of the wave and $\omega\tau$ represents the phase of the wave. After some amount of math and taking the limit as $\omega \to \infty$, we arrive at a form of the eikonal equation.

(5.4) $$\left|\nabla \tau\right|^2 = \frac{1}{c^2}$$

From this we can also derive the transport equation. This describes how the amplitude changes over the regime of the phase front.

(5.5)
$$2\nabla A \cdot \nabla \tau + A\nabla^2 \tau = 0$$

The transport equation and the eikonal equation can be solved by using multiple methods to give important information such as the time and distance a given ray travels [19]. Probably the most important result of the ray theory though is Snell's Law.

2. Snell's Law

Snell's law describes how a ray propagates in a medium with changing sound speed. This is especially helpful in modeling rays traveling through the stratified ocean since the sound speed in water changes due to pressure, temperature, and salinity. We define the sound speed of one region to be c_1 and the sound speed in a second region to be c_2. If we know a ray's angle of incidence onto the second medium θ_1 referenced to the horizontal then we know the angle θ_2 in which the refracted ray will propagate going through the second region [18].

(5.6)
$$\frac{cos(\theta_1)}{c_1} = \frac{cos(\theta_2)}{c_2}$$

Snell's law would seem to only work between regions of constant sound speed. However, any region with non-constant sound speed can be considered as an infinite amount of small layers with "constant" sound speeds. It can even be shown that as long as the changing sound speed is linear in the region of interest, a ray will propagate in a circular path with radius *R* related to the sound speed at the location of the ray's source, c_0, and the slope of the sound speed profile, *a* [18].

(5.7)
$$R = -\frac{c_0}{a}$$

Even with these results it would still be hard to calculate ray paths for media in which the sound speed is not varying linearly. However, computer programs can use the information we just derived to compute ray paths. As mentioned before, the program numerically quantizes the region of interest into many small layers of constant sound speed in order to approximate the ray path by using Snell’s Law.

B. PROPAGATION MODELING USING BELLHOP

Bellhop is a ray-tracing program that models acoustic pressure fields in any ocean environment. Given a sound speed profile, boundary conditions, bathymetry, and other information about the environment, it can produce graphs of transmission loss, eigenrays, ray arrivals, and received time series [20].

My goal of using Bellhop was to identify how much of a difference the depth of the sensor would impact communications to a sea floor node. The depth of these sea floor nodes is as much as 3000 meters. I used the Munk deep sea sound-speed profile to represent a deep-water ocean environment. The Munk profile is given by the following equation, where $c(z)$ is the sound speed as a function of depth [21].

$$c(z) = 1500\left[1.0 + \epsilon\left(\tilde{z} - 1 + e^{-\tilde{z}}\right)\right] \tag{5.8}$$

The scaled depth $\tilde{z}$ and the constant ϵ are given the following values.

$$\epsilon = 0.00737 \tag{5.9}$$

$$\tilde{z} = \frac{2\left(z - 1300\right)}{1300} \tag{5.10}$$

The resulting sound speed profile is shown in Figure 13.

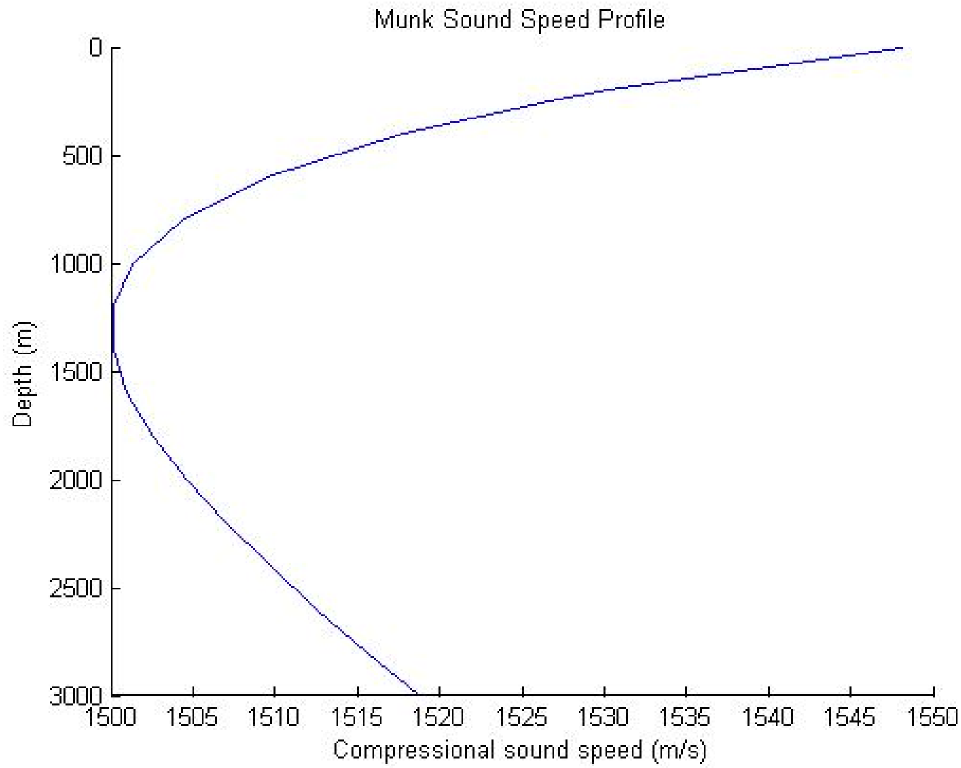

Figure 13. A 3000 m Munk sound-speed profile.

Next, I used Bellhop to generate ray traces for a sound source located at 0.25 meters depth and then at 7.0 meters depth. Once again, the goal was to see if there was an appreciable amount of ray path difference between the two locations. The Wave Glider can maintain a watch circle around a node of about 25 meters, but to be safe the results of the ray trace were graphed all the way up to 1000 meters to simulate communications between the Wave Glider and a bottom node that was farther away. Figure 14 is a graph of the ray tracing done with a source depth of 0.25 meters and Figure 15 has the source depth at 7 meters. The minimum and maximum launch angles relative to the horizontal axis were 55 and 89 degrees, respectively.

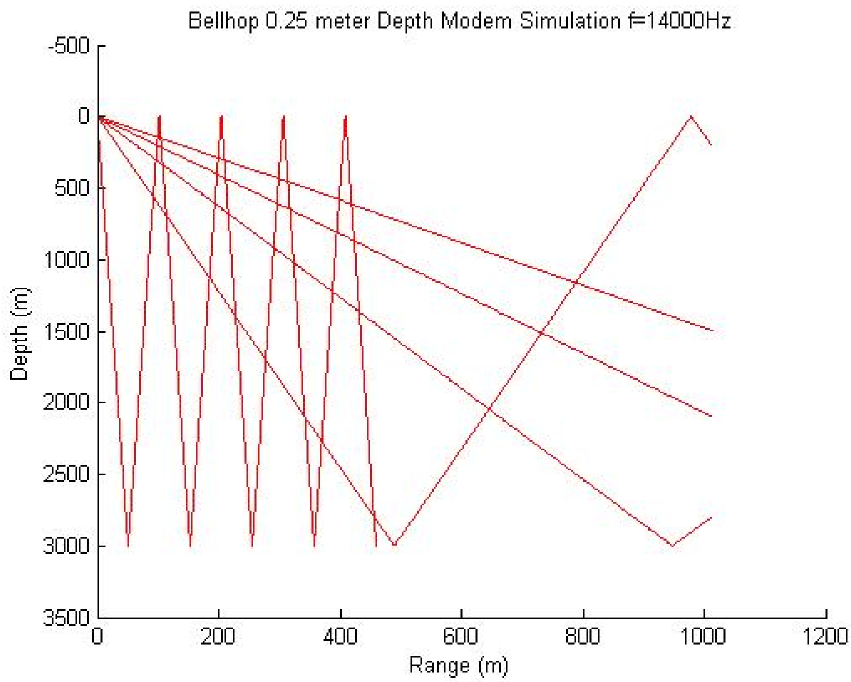

Figure 14. Ray tracing for a source at 0.25 m depth to a range of 1000 m

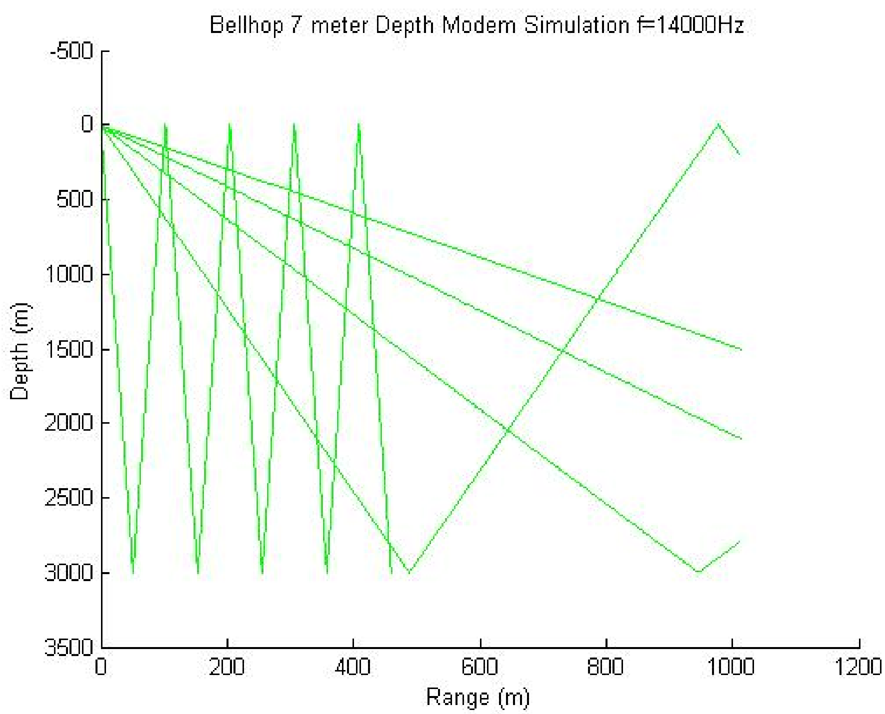

Figure 15. Ray tracing for a source at 7.0 m depth to a range of 1000 m

As we can see from the graphs, the depth made very little difference with respect to the propagation paths of acoustic rays from the modem. Next, I checked if the depth would make a difference in case the modem on the Wave Glider was to communicate with a node that was much further away than the closest node. I extended the maximum range calculated by Bellhop. Figure 16 is a graph of the ray tracing done with a source depth of 0.25 meters and Figure 17 with a source depth of 7 meters. Once again, the frequency used was 14kHz. The minimum launch angle was -10 degrees and the maximum launch angle was 10 degrees relative to the horizontal axis.

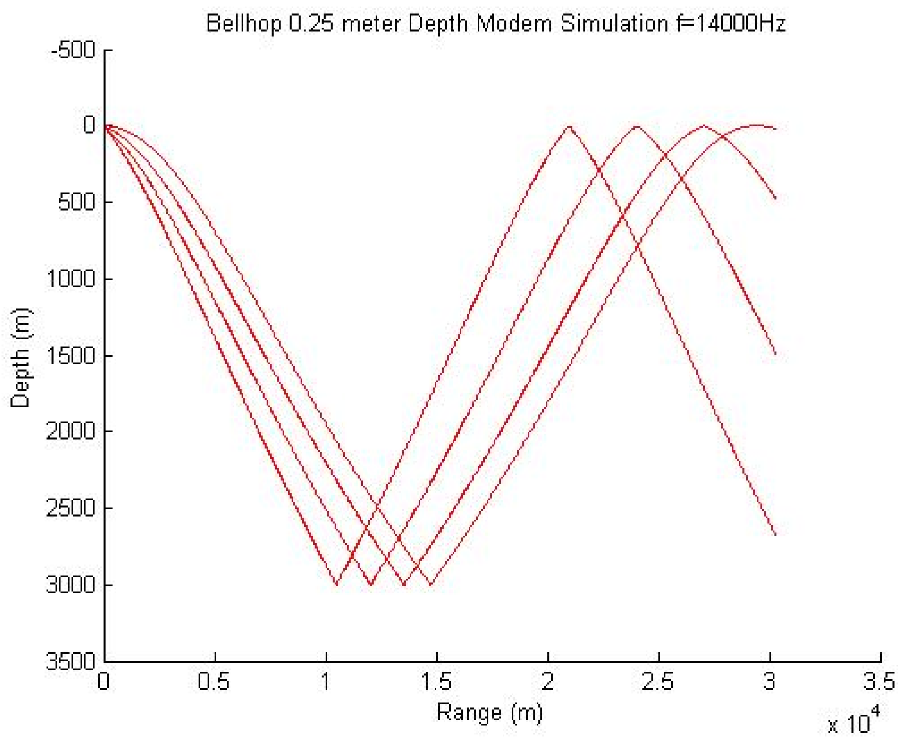

Figure 16. Ray tracing for a source at 0.25 m depth to a range of 30 km

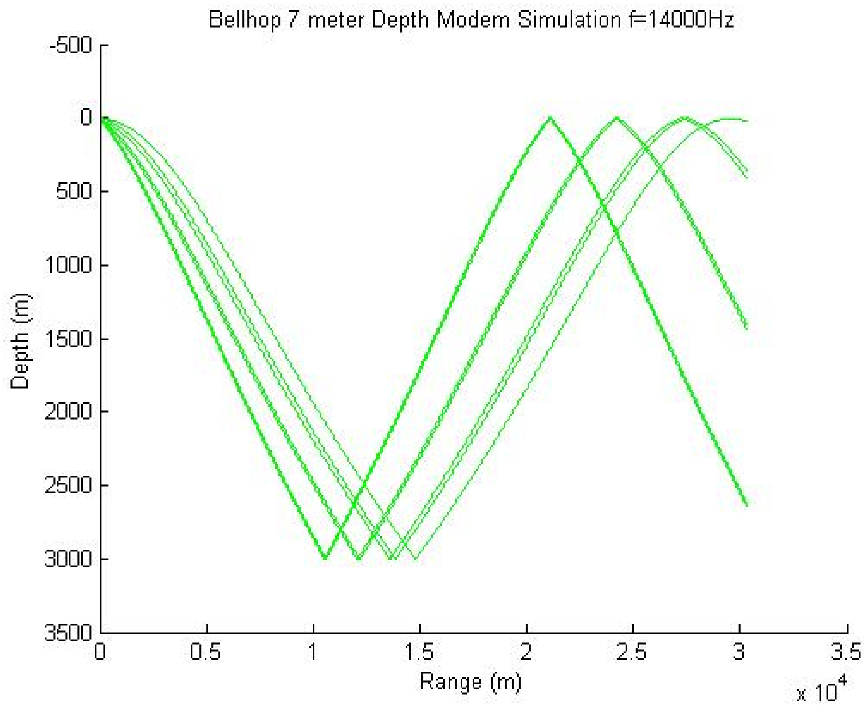

Figure 17. Ray tracing for a source at 7.0 m depth to a range of 30 km

Although it is hard to see, if we compare the two graphs closely, we can see that when the modem is at 7 meters of depth it is able to transmit a signal a little bit further without reflecting off of the bottom. This makes sense since a deeper source would be able to take advantage of the downward refracting sound speed profile more than one closer to the surface. This means that if we desire the Wave Glider modem to communicate to further away nodes, it would be advantageous to place the modem either on the glider portion or in a tow.

C. SHADOWING/INTERFERENCE OF GLIDER BODY

Some interference of the wave glider itself could occur if a piece of the vehicle were to lie in between the modem and the sea floor node that it is communicating with. This problem could only really exist if the modem was placed on the float portion of the vehicle since the glider body is the only part of the vehicle that could lie between the modem and the node. The glider portion of the vehicle tends to lead the float portion by 0.55 meters [6]. Using simple trigonometry we can calculate the horizontal distance the node would have to be from the float in order to cause an issue. Figure 18 shows the geometry of the float, glider, and sea floor node. It was found that the node would have to be 235 meters away from the float.

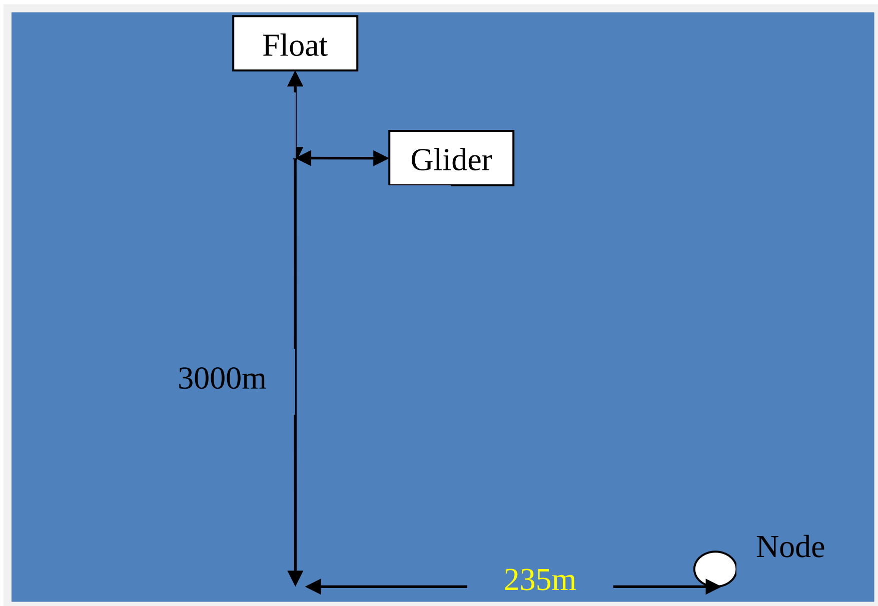

Figure 18. The distances involved with the glider interfering with the communication of a float mounted modem

At this distance and depth, the propagation angle of the signal would be 85 degrees relative to the horizontal. In this sound speed profile, the signal would propagate in a relatively straight line. Also if the Wave Glider wanted to communicate to further away nodes, the distances involved would be much greater than 235 meters. It should be noted however, that the blockage problem can be completely avoided if the modem were to be placed on the glider or on a tow body.

D. SUMMARY

In all aspects of our acoustic considerations, it would be more beneficial to have the modem away from the surface. If the Wave Glider modem is to communicate with far away nodes, a glider or tow body mounted modem could communicate to longer distances. Also a glider or tow-body mounted modem would completely avoid interference from the glider portion of the vehicle.

VI. NOISE

A. BACKGROUND

1. Noise Overview

The amount of noise associated with the candidate modem locations is an important consideration. If noise dominates communication in a particular integration scheme, then the signal-to-noise ratio (SNR) is degraded and the acoustic modem will not be able to effectively relay information without errors. The main criteria that we are looking for in examining noise is a high SNR. We can use the passive sonar equation to illustrate this.

$$SL - TL \geq NL - DI + DT \tag{6.1}$$

SL is the source level, *TL* is the transmission loss, *NL* is the noise level, *DI* is the directivity index, and *DT* is the detection threshold expressed in dB units. If we rearrange this equation differently, we can more clearly see the SNR.

$$SL - TL - (NL - DI) \geq DT \tag{6.2}$$

Since these are dB quantities, additions and subtractions correspond to multiplications and divisions, respectively. Here we can see that the signal transmitted to the modem after accounting for transmission loss must be greater than the noise by a certain amount referred to as our detection threshold [18].

Noise can be separated into different categories. An analysis of the ambient noise and the self noise associated with each location on the vehicle follows.

2. Ambient Noise

Ambient noise is defined as the noise that is not due to a hydrophone itself and/or its manner of mounting. In short, it is the noise due to the ocean environment itself. Ambient noise can come from different sources in the ocean and these different sources dominate at different frequency bands and vary with weather and sea state conditions.

Specifically, we are interested in noise in the spectral region around 10kHz, since the modems operate at around 10 kHz. Figure 19 shows that shipping noise is not of concern above 1 kHz [18].

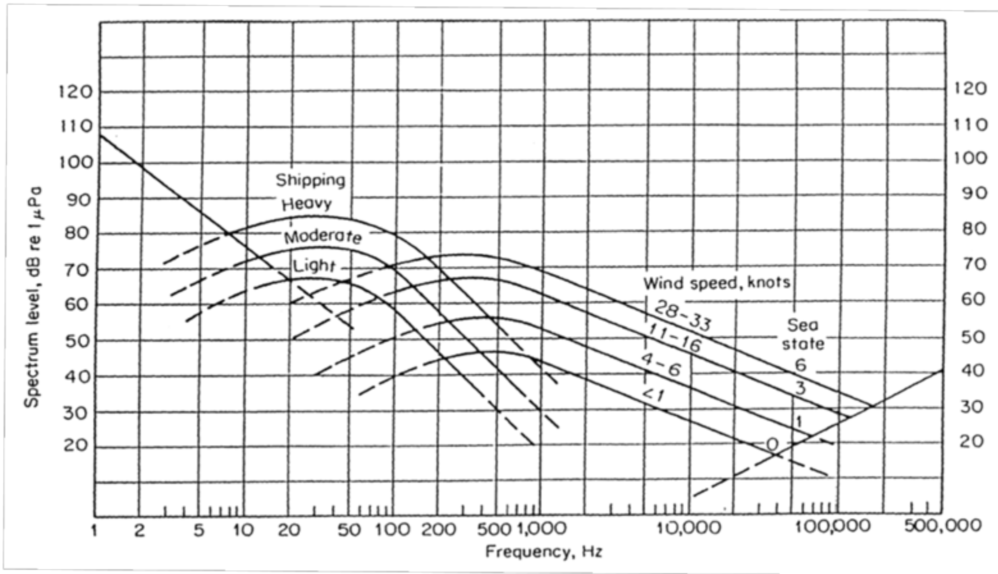

Figure 19. Sources of ambient noise in the ocean and their corresponding frequency ranges.

Most sources of the noise in this band originate at the sea surface and experience attenuation with depth, although usually the distance scales that people are have studied are much larger than the 7 meters we are looking to differentiate. Results also vary greatly with the geographic location in which the vehicle is operating in.

Some sources of ambient noise are completely unavoidable regardless of where the modem is placed, or vary only in small amounts relative to the depth of the modem. Examples include seismic disturbances, oceanic turbulence, thermal noise, and ship traffic. We will only examine the sources of noise that vary with the location of the modem on the Wave Glider, since this is the only variable we have control over [18].

B. ANALYSIS

1. Noise Due to Surface Waves

Noise from surface waves can affect the 0.5 to 25 kHz band, and is caused by the sea state and/or the wind forces on the surface of the water. Better correlations are known for wind speed than sea state simply because sea state is difficult to quantify. The exact process by which surface waves generate noise is not completely understood. However, a theory has been produced relating the period of surface waves to how quickly their pressure changes attenuate with respect to depth. This attenuation can be seen in Figure 20 [18].

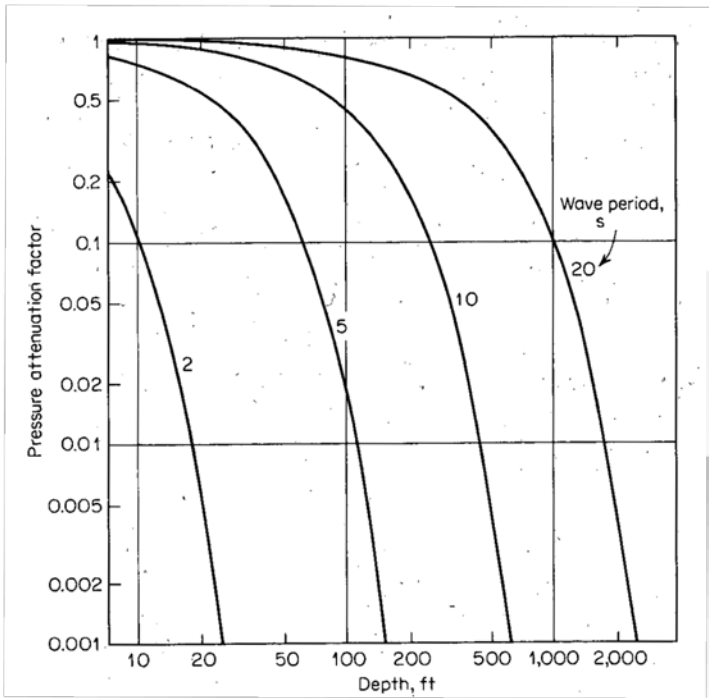

Figure 20. Attenuation of pressure changes due to surfaces waves at a given wave period and depth

As we can see from the graph, the pressure due to surface waves attenuates quite rapidly as the depth is increased and as the period of the waves is decreased. At the frequencies we are interested in, the noise due to surface waves will attenuate quickly with depth. Therefore, it is advantageous to place the acoustic modem at a depth of 7 meters as opposed to closer to the surface in order to benefit from the rapid attenuation of the surface wave noise with depth.

2. **Noise Due to Rain**

Rain can contribute an appreciable amount to the ambient noise spectrum in the frequencies that we are interested in. The magnitude of the effect can be attributed to the rate of the rainfall and the depth of the modem. Figure 21 shows the level of noise in the frequencies of interest [18].

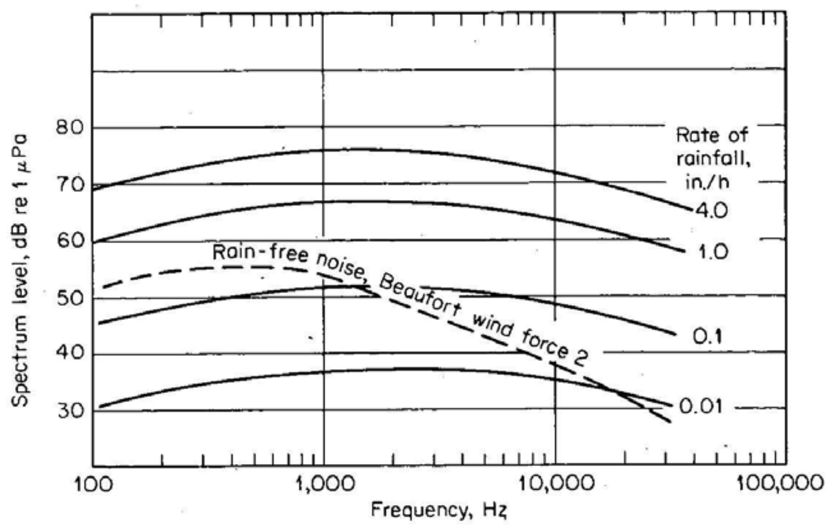

Figure 21. Spectrum levels of noise attributed to rain

If we consider each drop of water hitting the surface of water to be a hemispherical source, we can get an estimate to the transmission loss that the noise would experience going to an acoustic modem located 7 meters below the surface. Normally, the surface area of a spherically spreading source is given by the surface area of a sphere of radius R. However, we are dealing with a surface area of a hemisphere, so the surface area is halved.

(6.3) $$A_s = 2\pi r^2$$

The power passing through this surface is given by the integration of the intensity of the wave over this area.

(6.4) $$\Pi = \oint I \, dS = \frac{p_{rms}^2}{\rho_o c} 2\pi r^2$$

The total power remains constant as the sound passes through a surface r meters away.

(6.5) $$\Pi = \frac{p_{rms}^2(1m)}{\rho_o c} 2\pi(1m)^2 = \frac{p_{rms}^2(r)}{\rho_o c} 2\pi r^2$$

Therefore, the following ratio is true.

(6.6) $$\frac{p_{rms}(1m)}{p_{rms}(r)} = \frac{r}{1m}$$

Transmission loss is defined as

(6.7) $$TL = 20\log\left(\frac{p_{rms}(1)}{p_{rms}(r)}\right) = 20\log(r)$$

where the transmission loss is expressed in dB referenced to 1 meter. Coincidentally, this is the same as if we assumed spherical spreading. If we plug in a distance of 7 meters into this formula, we see that we get a transmission loss of 16.9 dB re 1m. Thus, if there is rain in the environment that the Wave Glider is operating in, the noise due to the rain would be greatly diminished if the modem is placed either on the lower body or a tow body.

3. Self-Noise of the Wave Glider

A full study of the self-noise due to the Wave Glider itself has not been completed. Due to the propulsion system of the vehicle being entirely wave actuated though, the noise of the vehicle would only be mechanical in nature. The only moving parts would exist on the lower body, and the noise due to these components would be proportional to the speed of the vehicle. The frequency band would also be related to the period of the waves and the sea state. Complete avoidance of the self-noise of the propulsive mechanisms of the vehicle though is recommended and could be achieved by either placing the modem on the float portion of the vehicle or the tow body.

C. SUMMARY

In all cases of our noise analysis, the tow body location is a favorable alternative to both the float and lower body locations. The tow body would avoid more of the noise at the surface than if it was mounted on the float portion, and it would avoid more of the self-noise of the vehicle than if it was mounted on the lower body. Once again, the differences in distance that we are analyzing are much smaller than many of the studies in noise that have been done, but regardless of how small the distance is, any advantage that the modem would get in SNR should be considered.

VII. CONCLUSIONS AND RECOMMENDATIONS

A. CONCLUSIONS

Although the estimated speed penalties seem low, the relationship between the values seems reasonable. In terms of minimizing drag, either the float or a tow body are viable options. For our acoustic analysis, the glider or tow body mounts would be able to communicate with further away nodes and would avoid the problem of possible interference with the glider body. Lastly, a float mounted modem would suffer from possible surface noise, while a glider mounted modem would be subject to the self-noise of the propulsive fins on the glider. A modem mounted on the tow body would minimize these noise sources.

From the results in this study, a tow body would be the preferable location because of our acoustic and noise related considerations. The drag is worse than the float mounted case; however, since we are integrating an acoustic modem it is more important that the modem is able to communicate effectively. The tow body mount also avoids possible interference with the propulsive mechanisms of a glider-mounted modem.

The results in this thesis seem to agree with other tests that have been done on acoustic modem integration with the Wave Glider. In one particular test, a modem's performance was compared in different positions on the Wave Glider. One integration was on the glider body and the other was on the float body. In both of these cases, the modem demonstrated effective communications with its target to within 2.5 km. However, it was noted that the speed of the vehicle was impacted heavily when integrating the modem with the glider body [22].

B. RECOMMENDATIONS

This analysis was all theory based and many approximations were made in deriving the results, especially those of the drag analysis. Obtaining more data on the relationship between Wave Glider velocity and wave height would make calculating the power available to the Wave Glider more accurate. It would also be extremely helpful for this study to acquire velocity and drag data for the Wave Glider from flow tank experiments. Lastly, quantifying the self-noise of the Wave Glider in different sea state conditions would help identify the impact it would have on a receiver located on the Glider.

This thesis did not examine the possibility of separating the transmitter and receiver portions of the modem to different locations. An in-depth analysis of this integration scheme should be considered in future studies.

LIST OF REFERENCES

[1] J. A. Rice. “Seaweb acoustic communication and navigation networks,” in *Proceedings of the International Conference Underwater Acoustic Measurements: Technologies & Results*, Heraklion, Greece, 2005.

[2] J. A. Rice, “Gatekeeper Station-Keeping Gateway Buoy,” *SBIR Topic N05–077*, Office of Naval Research Report, San Diego, CA, 2005.

[3] G. O. Pickens. “Wave-Actuated Horizontal Array Stretcher.” U.S. Patent 3,872,819, March 1975.

[4] R. Hine, S. Willcox, G. Hine, and T. Richardson. “The Wave Glider: A wave-powered autonomous marine vehicle,” in *OCEANS 2009, MTS/IEEE Biloxi – Marine Technology for our Future: Global and Local Challenges*, 2009, pp. 1–6, 26–29.

[5] J. Mullison, D. Symonds, and N. Trenaman. “ADCP data collected from a liquid robotics wave glider,” in *Proceedings of the IEEE/OES/CWTM Tenth Working Conference on Current Measurement Technology*, 2011, pp. 266–272.

[6] N. Kraus, and B. Bingham. “Estimation of Wave Glider dynamics for precise positioning,” in *Oceans 2011*, pp. 1–9.

[7] C. Greene, A Packer, and H. Dorn. “Dual frequency echosounder testing,” [white paper], Liquid Robotics, Cornell University, and BioSonics, Apr. 2012.

[8] B. R. Munson, D. F. Young, T. H. Okiishi and W. W. Huebsch, *Fundamentals of Fluid Mechanics* 6th ed. Hoboken, NJ: John Wiley & Sons, 2009.

[9] S. F. Hoerner, *Fluid-Dynamic Drag: Practical Information on Aerodynamic Drag and Hydrodynamic Resistance*. Midland Park, NJ: S.F. Hoerner, 1965.

[10] M. M. Zdravkovich, V. P. Brand, G. Mathew, and A. Weston. “Flow past short circular cylinders with two free ends.” *Journal of Fluid Mechanics*, vol. 203, pp. 557–575, 1989.

[11] J. A. Rice. “Report on Preliminary WAHAS Tests,” Naval Ocean Systems Center Test Report, Mar. 1982.

[12] T. K. A. Brekken, H. T. Ozkan-Haller, and A. Simmons. “A methodology for large-scale ocean wave power time-series generation.” *IEEE Journal of Oceanic Engineering*, vol. 37, no. 2, pp. 294–300, 2012.

[13] F. Monaldo. “Measurement of wave crest length and groupiness from spaceborne synthetic aperture radar.” *Marine Structures*, vol. 13, no. 4–5, pp. 349–366, 2000.

[14] N. Scott, T. Hara, P. A. Hwang, and E. J. Walsh. “Directionality and crest length statistics of steep waves in open ocean waters.” *Journal of Atmospheric and Oceanic Technology*, vol. 22, pp. 272–281, 2004.

[15] D. A. Read, F. S. Hover, and M. S. Triantafyllou. “Forces on oscillating foils for propulsion and maneuvering.” *Journal of Fluids and Structures*, vol. 17, pp. 163–183, 2002.

[16] J. A. Sparenberg. *Elements of Hyrdodynamic Propulsion*. The Hague: Martinus Nijhoff Publishers, 2012.

[17] “Executive Summary of SHARC-TAIL Tests on March 19th 2012,” Liquid Robotics Executive Summary, Kawaihea, HI, Mar. 2012.

[18] R. J. Urick. *Principles of Underwater Sound for Engineers*. New York: McGraw-Hill, 1975.

[19] K. Smith. “Solving the wave equation in more general environments: Ray methods.” PH4455 Class Notes, pp. 100–103, Naval Postgraduate School, Spring quarter.

[20] M. B. Porter. *The Bellhop Manual and Users Guide*. Heat, Light, and Sound Research, Inc., La Jolla, CA, 2011.

[21] W. H. Munk. “Sound channel in an exponentially stratified ocean with applications to SOFAR.” *Journal of the Acoustical Society of America*, vol. 55, no. 2, pp. 220–226, 1974.

[22] G. Hine. “Underwater Acoustic Modem Test Report,” Liquid Robotics Gateway Project Test Report, Kamuela, HI, Jul. 2010.

INITIAL DISTRIBUTION LIST

1. Defense Technical Information Center
   Ft. Belvoir, VA

2. Dudley Knox Library
   Naval Postgraduate School
   Monterey, CA

3. Joseph Rice
   Department of Physics
   Naval Postgraduate School
   Monterey, CA

4. RADM (Ret.) Winford G. Ellis
   Chair, Undersea Warfare
   Director, Undersea Warfare Research Center
   Naval Postgraduate School
   Monterey, CA

5. LT Tim Rochholz
   Naval Postgraduate School
   Monterey, CA

6. Dave Jackson
   Office of Naval Intelligence
   Suitland, MD

7. Chris Fletcher
   Space and Naval Warfare Systems Center Pacific
   San Diego, California

8. Ryan Carlon
   Liquid Robotics, Inc.
   Sunnyvale, CA

9. Scott Willcox
   Liquid Robotics, Inc.
   Sunnyvale, CA

10. Joseph Beach
    Naval Postgraduate School
    Monterey, CA